**A METHOD OF ESTIMATING TRANSIENT-CAVITY DIAMETERS FOR IMPACT CRATERS FORMED IN DRY SAND.** M.J. Cintala,[1] O.S. Barnouin-Jha[2], and F. Hörz[1]. [1]Code SR, NASA Johnson Space Center, Houston, TX 77598 (Mark.J.Cintala@nasa.gov); [2]The Johns Hopkins Applied Physics Laboratory, Johns Hopkins Road, Laurel, MD 20723.

**Introduction:** Analyses of impact craters formed in laboratory experiments historically have been the source of many fundamental observations and interpretations of the impact-cratering process itself.[1,2,3] Due to its ready availability, ease of handling, and lack of strength, dry sand of various types has been the target material of choice in the majority of such experiments. A consequence of its lack of intrinsic strength, however, is dry sand's inability to maintain slopes above its angle of repose. Evidence from field observations of simple terrestrial craters[4,5] and laboratory craters formed in more cohesive granular media[6] suggests that transient cavities are similar to paraboloids in shape. Cross-sections of craters formed in dry sand, however, are nearly conical with the wall slopes at or near the angle of repose, indicating that the original crater form has been modified by one or more processes, among which is simple slope failure. Because the dimensions and shape of the transient cavity reflect the detailed conditions of a given impact event, its characterization has long been a desired goal in experimentation. A means of estimating the position of the transient cavity's rim is suggested below, relying on determination of velocities of material ejected from the growing cavity.

**Approach:** The method used here is founded on the observation that parabolic trajectories described by grains of sand ejected in laboratory-scale impacts *in vacuo* are, for the most part, relatively well-defined and orderly, even in cases involving very coarse-grained targets (Fig. 1).[7] It is clear from the figure that fragments are ejected at decreasing speeds as the location of the final crater's rim crest is approached. Indeed, as the ejection speeds drop, the parabolic trajectories become smaller and smaller, with the result that the last, slowest piece of material to be ejected, describing the limiting case, would barely leave the cavity to be deposited on the top of the rim crest. Thus, by plotting the point at the a number of parabolic trajectories, the location of the transient cavity's rim crest should be approached as the elevations of the parabolic maxima approach the target surface.

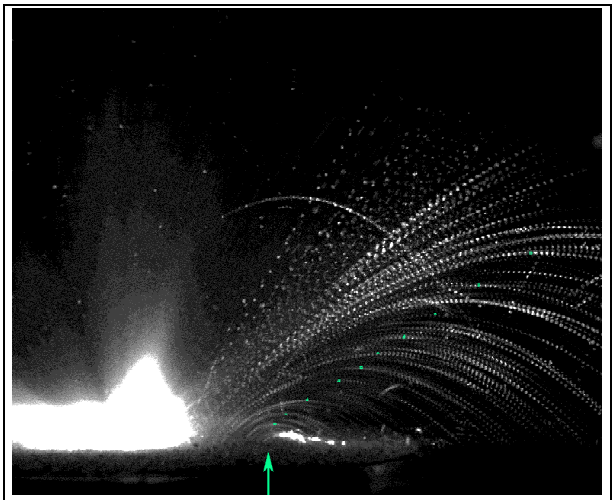

Figure 1. Stroboscopic photograph of ejecta in flight from a crater formed in coarse sand by the impact of a 4.76-mm aluminum sphere at 0.802 km $s^{-1}$, illustrating how the maxima of the parabolic trajectories approach the rim of the growing cavity (whose location in the horizontal dimension is approximated by the arrow) as ejection speeds decrease. A few such maxima are indicated in green.

**An example:** This method can be illustrated by use of an existing dataset that describes seven impacts of 4.76-mm aluminum spheres into targets of blasting sand, with grain dimensions of 1-3-mm.[7] The trajectory data for these impacts can be used to derive the *x*-*y* coordinates at which the of maxima of all the measured parabolic trajectories occur; the origin of the coordinate system is the impact point itself, and the x-axis lies along the pre-impact target surface. An example of the trend resulting from such measurements is given in Fig. 2

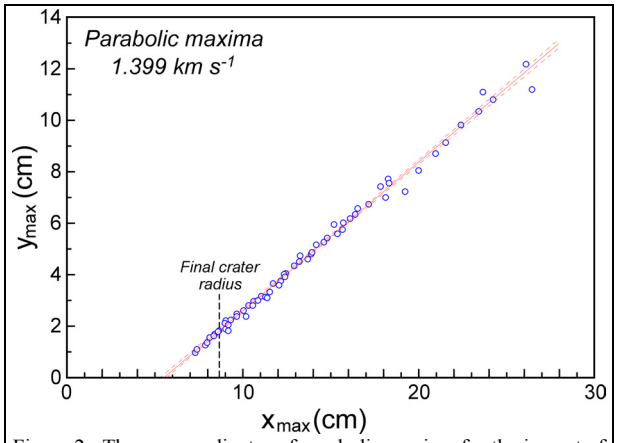


Figure 2. The *x*-*y* coordinates of parabolic maxima for the impact of an aluminum sphere into coarse-grained blasting sand. Only trajectories originating outward of 0.4 final-crater radii were used in this plot. The dashed curves around the fit represent the 95% confidence band.

Ideally, all of the trajectories close to the rim of the final crater would be measured, increasing the accuracy of the fit near the crater and permitting determination of the location of the cavity's rim directly from

plots like Fig. 2. In this case, however, the rate at which the illuminating laser was flashed was constant, and too rapid to resolve individual images of the slower fragments; this prevented precise fitting of trajectories to the lower-speed fragments.[7] Variable illumination rates would be necessary to image an entire event fully, and indeed the prospect of doing so is part of the impetus for locating and being able to predict the time of formation of the transient cavity. In any event, the curve in Fig. 2 cannot yet be used to estimate the position of the cavity's rim; the curve cannot simply be extrapolated to zero elevation ($y$=0), because the final parabola had to clear the rim of the transient cavity, which is modestly higher than that of the final crater.

While only the diameters of the craters in the dataset of [*7*] were measured, they were similar in geometry to those formed in finer-grained sand.[8] A fit to rim-height as a function of final-crater diameter for 29 such craters yields

$$R_e = 0.055 D_r^{0.73} \quad (1)$$

in which $R_e$ is the rim height and $D_r$ is the rim-crest diameter of the final crater. The small number of craters over a relatively narrow diameter range gives a value of $r^2$ of 0.69 for this fit, but in the spirit of this technique description, it is not a major problem. The final crater created by the impact described in Fig. 2 had a diameter of 16.7 cm; use of this value in eq. (1) gives a rim height for the final crater of 0.43 cm. Using this for the minimum value of $y_{max}$ in the fit illustrated in Fig. 2 yields a corresponding value for $x_{max}$ of 6.22 cm. With a final radius of 8.35 cm, this value implies a post-excavation enlargement of 2.13 cm, or 34%. The rim crest of the transient cavity before its modification was certainly higher than that of the final crater; this, coupled with inspection of Fig. 2, shows that the value of 6.22 cm for the cavity radius is a minimum estimate. A simple maximum can be determined from the figure by assuming that the smallest parabola represented the last fragment out of the crater. The value of $x_{max}$ thus obtained is 7.36 cm, yielding a post-excavation enlargement of 0.99 cm, or 13%.

**Discussion:** The example described above is far from ideal, in that the statistical variances caused by the coarseness of the target material have been shown to be large.[7] Nevertheless, even with this target material and the assumptions and approximations used to estimate the horizontal dimension of the event's transient cavity, the results are very promising. It is interesting that even the lower value for the cavity's horizontal enlargement is greater than those suggested for simple terrestrial craters on the basis of model reconstructions; enlargement at Brent, for instance, has been estimated at 10%.[9] Conversely, even the lower value of 13% bracketed here is certainly too small, as there are even smaller parabolic trajectories visible in the photograph.

This method holds considerable promise for the future determination of transient-cavity diameters. Specifically, finer-grained target materials will minimize the variance in ejection speed and angle observed in the case of the coarse-sand targets, permitting even better fits than in Fig. 2. In addition, an iterative approach to illumination of the ejecta will provide much better time resolution for the lower-speed ejecta, leading to the prospect of direct determination of the cavity's radius. The determination of a transient-cavity diameter and its difference relative to that of the final observed crater are important for estimating the forces that both cause and prevent failure of a transient crater. The methodology described here might allow, for example, direct estimation of the dynamic shear strength of the granular target during catering, which is not easily determined by standard static soil measurement techniques.[10] Such estimates can provide new insights into how target strength and frictional processes influence the modification of craters immediately after excavation.

**References:** ***1*** D.E. Gault *et al.* (1968) in *Shock Metamorphism of Natural Materials* (Mono Books), p. 87. ***2*** W.L. Quaide and V.R. Oberbeck (1968) *JGR* **73**, 5247. ***3*** P.H. Schultz and D.E. Gault (1985) *JGR* **90**, 3701. ***4*** M.R. Dence (1973) *Meteoritics* **8**, 343. ***5*** P.B. Robertson and R.A.F. Grieve (1977) in *Impact and Explosion Cratering* (Pergamon Press), p. 687. ***6*** P.H. Schultz (1992) *JGR* **97**, 11623. ***7*** M.J. Cintala *et al.* (1999) *MAPS* **34**, 605. ***8*** M.J. Cintala *et al.* (1999) *Lunar Planet. Sci XXX*, abstract 1958. ***9*** R.A.F. Grieve and M.J. Cintala (1981) *Proc. Lunar Planet. Sci. Conf. 12B*, 1607. ***10*** S.B. Savage (1984) *Advances in Applied Mechanics 24*, (Academic Press), 289.